

X-ray structural investigation of the oxyvanite (V_3O_5) – berdesinskiite (V_2TiO_5) series: V^{4+} substituting for octahedrally coordinated Ti^{4+}

THOMAS ARMBRUSTER^{1,*}, EVGENY V. GALUSKIN², LEONID Z. REZNITSKY³ and EVGENY V. SKLYAROV³

¹ Mineralogical Crystallography, Institute of Geological Sciences, Freiestr. 3, University of Bern, 3012 Bern, Switzerland

*Corresponding author, e-mail: armbruster@krist.unibe.ch

² Department of Geochemistry, Mineralogy and Petrography, Faculty of Earth Sciences, University of Silesia, Będzińska 60, 41-200 Sosnowiec, Poland

³ Institute of the Earth's crust (IZK) SB RAS, 664033 Irkutsk-33, Russia

Abstract: The crystal structures of three different solid-solution members between the new mineral oxyvanite (V_3O_5) – and berdesinskiite (V_2TiO_5) from a quartzite rock in the Pereval marble quarry of the Sludyanka complex, south of Lake Baikal (Russia), have been refined in space group $C2/c$ ($a \approx 10.0$, $b \approx 5.0$, $c \approx 7.0$ Å, $\beta \approx 111^\circ$) from X-ray single-crystal diffraction-data. The composition of the studied crystals, determined by electron-microprobe analyses, is: $(V_{1.67}^{3+}Cr_{0.33}^{3+})(V_{0.59}^{4+}Ti_{0.41}^{4+})O_5$, $(V_{1.67}^{3+}Cr_{0.33}^{3+})(V_{0.46}^{4+}Ti_{0.54}^{4+})O_5$, and $(V_{1.38}^{3+}Cr_{0.61}^{3+})(V_{0.24}^{4+}Ti_{0.76}^{4+})O_5$. The common structure type of oxyvanite and berdesinskiite can be described by hexagonal closest oxygen packing with 3/5 of the octahedral voids occupied. Site-occupancy refinements support previous studies on synthetic V_2TiO_5 and V_3O_5 indicating that a strongly distorted octahedrally coordinated site, forming pairs of face-sharing octahedra, is 1:1 occupied by M^{3+} and M^{4+} (Ti^{4+} , V^{4+}) whereas a more regular octahedral site is only occupied by M^{3+} (V, Cr).

Key-words: oxyvanite, V_3O_5 , berdesinskiite, V_2TiO_5 , crystal structure, single-crystal X-ray diffraction, vanadium valence, V^{3+} , V^{4+} .

1. Introduction

Electron microprobe and SEM (Scanning Electron Microscope) energy-dispersive analyses were carried out on separated high-density minerals from diopside-rich quartzite rocks of the Pereval marble quarry in the Sludyanka complex, belonging to one of the metamorphic terranes (maximum P,T conditions: $T = 800$ – 830 °C, $P = 6$ – 8 kbar) of the Central Asian fold belt. The terrain is situated to the south of Lake Baikal near the boundary with the Siberian craton.

Analytical results of the high-density minerals, which were xenomorphic, dark red-black in color and between 0.05 and 0.2 mm in dimension, yielded a highly surprising ternary oxide composition within the system Ti–V–Cr–O. Using most frequent and common metal valences, the composition of the crystals could be described by a pseudo-binary series between TiO_2 and $(V,Cr)_2O_3$. Four different compositional groups were distinguished according to their TiO_2 content:

- (I) TiO_2 13–15 wt%
- (II) TiO_2 18–19 wt%
- (III) TiO_2 25–26 wt%
- (IV) TiO_2 51–54 wt%

The remaining components were V_2O_3 and Cr_2O_3 with trace concentrations of Fe_2O_3 , Al_2O_3 and MgO . At this stage it was assumed that these xenomorphic crystals represent various natural Magnéli-Andersson phases (Andersson *et al.*, 1959) of the series $(V,Cr)_2Ti_{n-2}O_{2n-1}$, the structures of which are closely related to that of rutile TiO_2 or α - PbO_2 and may be derived from them by crystallographic shear. However, X-ray single-crystal structure analyses for several representative samples of each group yielded for crystals from group (I) to (III) in all cases the monoclinic cell $a = 10.0$, $b = 5.0$, $c = 7.0$ Å, $\beta = 111^\circ$ of space group $C2/c$ characteristic of the mineral berdesinskiite, $V_2^{3+}TiO_5$, known from a strongly weathered gneiss near Lasamba Hill, Kenya (Bernhardt *et al.*, 1983). However, stoichiometric berdesinskiite (Bernhardt *et al.*, 1983) has 34.8 wt% TiO_2 . How can the strongly varying and decreased TiO_2 concentration be explained for a mineral of the berdesinskiite structure type?

The mineral representing the most TiO_2 -rich group (IV) was identified as schreyerite, $V_2^{3+}Ti_3O_9$ (Döbelin *et al.*, 2006), which has according to its stoichiometric formula 61.5 wt% TiO_2 . This theoretical value is contrasted by ca. 52 wt% TiO_2 analyzed for schreyerite from the southern shore of Lake Baikal, Russia. Our previous study (Döbelin

et al., 2006) indicated that vanadium occurs at this locality as V^{3+} and V^{4+} with V^{4+} substituting for Ti^{4+} . Another mineral from the same locality with V^{4+} partially replacing Ti^{4+} is batisivite, $V_8^{3+}TiO_6[BaSi_2O_7]O_{22}$, a member of the derbylite group (Armbruster *et al.*, 2008; Reznitsky *et al.*, 2008). This substitution is also evident for the minerals of the berdesinskiite structure-type. Thus, the varying composition from group (I) to (III) may be described by a solid-solution series between V_3O_5 and $V_2^{3+}TiO_5$ allowing for partial substitution of V^{3+} by Cr^{3+} . Experimental work by Schuiling & Feenstra (1980) already suggested that V^{4+} is rather common in minerals when the oxygen fugacity is close to that defined by the magnetite-hematite equilibrium. Under such conditions, vanadium changes its valence to 4+, and proxies mostly for Ti^{4+} , in ilmenite-hematite solid-solution members or rutile. More recently, Papike *et al.* (2004) determined the oxygen fugacity for V-bearing chromites and found that V^{3+} and V^{4+} occur in equal proportions in a basaltic melt with $\log fO_2$ halfway between the iron-wuestite and the quartz-fayalite-magnetite buffer.

V_3O_5 is known as a synthetic phase in the V–O phase diagram (Wriedt, 1989) and has a structure (Åsbrink, 1980; Hong & Åsbrink, 1982a) closely related to $V_2^{3+}TiO_5$ (berdesinskiite). The natural analogue of V_3O_5 has recently been submitted to *IMA CNMNC* as new mineral species, named oxyvanite. Species status and name have been approved (Reznitsky *et al.*, in press).

The present study provides a structural description of the solid-solution members between oxyvanite and berdesinskiite. Actually, the structure of berdesinskiite has not been published for a crystal of composition V_2TiO_5 , but has been assumed to be analogous to Fe_2TiO_5 (Drofenik *et al.*, 1981), based on corresponding unit-cell dimensions and symmetry. Åsbrink *et al.* (1986) cite a paper in preparation by Åsbrink & Sävborg (1986) dealing with X-ray and neutron powder refinements of the structure of synthetic V_2TiO_5 . However, this study has obviously never been published. In addition, Kolitsch & Tillmanns (2004) report in an abstract the structure refinement of type-locality berdesinskiite but detailed results are not available yet.

2. Experimental methods

One crystal each of group (I) and (II) but two crystals of group (III) were structurally analyzed using either an Enraf-Nonius CAD4 single-crystal diffractometer (equipped with scintillation counter) or a Bruker SMART 1K system equipped with a CCD detector. On both machines graphite-filtered Mo radiation was employed. For better direct comparison, cell dimensions of all crystals were measured with CAD4 by the same procedure from the scattering positions of 25 reflections with $33^\circ > \theta > 13^\circ$. Experimental details are listed in Table 1. For CAD4 intensity measurements data reduction, including background, Lorentz and

Table 1. Parameters for X-ray data collection and crystal-structure refinement.

Sample	I-2-7	II-7-21	III-7-22	III-9-11
Diffractometer	Enraf-Nonius CAD4	Enraf-Nonius CAD4	Bruker CCD 1K	Bruker CCD 1K
X-ray radiation (Å)	MoK α (0.71073)	MoK α (0.71073)	MoK α (0.71073)	MoK α (0.71073)
X-ray power	50 kV, 40 mA	50 kV, 40 mA	50 kV, 40 mA	50 kV, 40 mA
Temperature	293 K	293 K	293 K	293 K
Space group	C2/c (No. 15)	C2/c (No. 15)	C2/c (No. 15)	C2/c (No. 15)
Cell dimensions (Å)	10.0299(14), 5.0505(3), 6.999(2)	10.0546(12), 5.0603(5), 7.0111(10)	10.033(2), 5.039(6), 6.988(2)	10.0448(10), 5.0393(4), 6.9890(7)
β (°)	111.13(2)	110.845(10)	111.50(2)	111.486(9)
V (Å ³)	330.69(13)	333.37(7)	328.7(2)	329.19(6)
Z	4	4	4	4
Collection mode	Omega scan	Omega scan	Omega scan hemisphere	Omega scan hemisphere
Reflections collected	1316	1744	917	920
Max. 2 θ	69.8	69.8	55.4	55.7
Index range	$-16 \leq h \leq 16$ $-1 \leq k \leq 8$ $-3 \leq l \leq 11$	$-16 \leq h \leq 15$ $-8 \leq k \leq 8$ $-1 \leq l \leq 11$	$-8 \leq h \leq 13$ $-6 \leq k \leq 6$ $-8 \leq l \leq 8$	$-13 \leq h \leq 12$ $-6 \leq k \leq 6$ $-9 \leq l \leq 7$
Unique reflections	718	726	718	718
Reflections > 2 σ (I)	515	527	341	265
R_{int}	0.018	0.020	0.069	0.046
R_{σ}	0.025	0.024	0.039	0.032
Number of least squares parameters	40	40	40	26
Goof	1.096	1.042	1.229	0.982
$R1, I > 2\sigma(I)$	0.024	0.023	0.030	0.027
$R1, all data$	0.045	0.040	0.034	0.036
$wR2$ (on F^2)	0.071	0.072	0.099	0.069
$\Delta\rho_{min}$ ($e\text{Å}^{-3}$)	1.1 Close to V2	0.9 Close to V2	0.8 Close to V2	1.0 Close to V2
$\Delta\rho_{max}$ ($e\text{Å}^{-3}$)	0.9 Close to V1	0.8 Close to V1	0.6 Close to O3	0.5 Close to V2

polarization corrections and an empirical absorption correction based on ψ scans, was done using the SDP program library (Enraf-Nonius, 1983). As indicated by systematic absences, the structure was solved in space group *C2/c* by direct methods and refined using the program SHELX-97 (Sheldrick, 1997). Refinements were done with anisotropic displacement parameters for all sites. The refined chemical composition was constrained to the ideal composition of V₃O₅ because the scattering factors of Ti⁴⁺, V³⁺, V⁴⁺ and Cr³⁺ are very similar. CCD data were reduced using Bruker SAINT integration software. In contrast to CAD4 data, which were collected up to $\theta = 35^\circ$, SMART data were limited to $\theta_{\max} = 28^\circ$. Thus, the number of observations for SMART data decreased and for one crystal oxygen displacement-parameters were refined with the isotropic model to reduce the number of refined parameters. Test refinements were performed with unconstrained V occupancies for V1 (Wyckoff site 4a) and V2 (Wyckoff site 8f).

After X-ray data collection the studied crystals were embedded in epoxy resin, polished, and carbon-covered for electron-microprobe analyses. Mineral compositions were investigated by means of a CAMECA SX-100 microprobe operated at 15 kV and 20 nA, beam diameter 1–2 μm . The following standards, analytical lines, and analyzer crystals were used: diopside – MgK α (TAP); orthoclase – AlK α (TAP), rutile – TiK α (LIF), Cr₂O₃–CrK β (PET), Fe₂O₃–FeK α (LIF), metallic V–VK α (LIF). Concentrations of Si, Nb, Ta, W etc. are below the detection limit. Special care was taken to distinguish and resolve the characteristic radiations of Ti, V and Cr, as these transition metals coexist as main elements in the analyzed crystals. Analytical results for the crystals

I-2-7, II-7-21 and III-9-11 are given in Table 2. Crystal III-7-22 was lost but according to SEM-EDS analyses its composition was similar to crystal III-9-11.

3. Results

All refined crystal structures (*R1* between 2.3 and 3.0 %, see Table 1) are isotopic to synthetic Fe₂TiO₅ (Drofenik *et al.*, 1981), V₃O₅ (Hong & Åsbrink, 1982a), Ti₃O₅ (Hong & Åsbrink, 1982b), and CrTi₂O₅ (Müller-Buschbaum & Bluhm, 1988). For our refinements we have chosen the *C2/c* setting of space group No. 15, as suggested by Bernhardt *et al.* (1983) for berdesinskiite. However, the structures of synthetic high-temperature V₃O₅ (Hong & Åsbrink, 1982a) and Ti₃O₅ (Hong & Åsbrink, 1982b) have been described in *I2/a* setting. With all metal sites modeled by V scattering factors and allowing for unrestrained site-occupancy refinement, occupancy of V2 (Wyckoff site 8f) decreased for all samples significantly to 0.97 whereas the occupancy of V1 (Wyckoff site 4a) remained within three esd's at 1.0. Site occupancy of vanadium (23 electrons) of 0.97 corresponds to 22.3 electrons, indicating that a lighter element (Ti: 22 electrons) may also be concentrated on V2. Chemical compositions are summarized in Table 2. In the final refinement cycles all metal sites were fixed at complete V occupancy to reduce correlation effects. Atomic coordinates and anisotropic displacement parameters are summarized in Tables 3 and 4. M–O distances are listed in Table 5.

4. Discussion

Chemical and structural data suggest that the analyzed minerals represent Cr³⁺-bearing members of the V₃O₅ (oxyvanite)–V₂TiO₅ (berdesinskiite) solid-solution series characterized by substitution of Ti⁴⁺ by V⁴⁺. The crystal structure of synthetic low-, high-V₃O₅, and the new mineral oxyvanite can be described as a hexagonal closest packing of oxygen atoms [layers parallel to (20 $\bar{1}$)] with 3/5 of the octahedral interstices occupied by V³⁺ and V⁴⁺. V-centered octahedra form edge-connected chains, which run parallel to [010]. These chains have a central backbone of M1O₆ octahedra (multiplicity 4) alternating with pairs of M2O₆ octahedra (multiplicity 8) having shared edges with M1O₆ octahedra. These M1–M2 chains have been named before “berdesinskiite-like chains” (Döbelin *et al.*, 2006) and are considered building blocks (*P*-slabs) of a polysomatic series together with α -PbO₂-like octahedral chains (*Q*-slabs). The structure of the mineral schreyerite, V₂Ti₃O₉, may be described as a *PQ* polysome of this series. Berdesinskiite- or V₃O₅-like chains form also a modular unit of the batisivite structure (Armbruster *et al.*, 2008) occurring at the same locality as berdesinskiite, oxyvanite, and schreyerite (Reznitsky *et al.*, 2008).

Table 2. Composition of analyzed oxyvanite-berdesinskiite solid-solution members; formulae normalized to 3 cations and 5 O.

	I-2-7	II-7-21	III-9-11
	Mean of 6	Mean of 4	Mean of 7
V ₂ O ₃ ^a	53.93	54.21	44.44
VO ₂ ^a	21.25	16.66	8.82
Fe ₂ O ₃	0.04	0.37	0.04
TiO ₂	14.02	18.78	26.12
Cr ₂ O ₃	10.76	10.80	19.96
MgO	0.02	0.02	0.08
Al ₂ O ₃			0.12
Total	100.02	100.84	99.58
V ³⁺	1.669	1.661	1.375
V ⁴⁺	0.001	0.001	0.005
Cr ³⁺	0.328	0.326	0.609
Fe ³⁺	0.001	0.011	0.001
Al			0.005
Mg	0.001	0.001	0.005
	2	2	2
Ti ⁴⁺	0.407	0.540	0.758
V ⁴⁺	0.593	0.460	0.242
	1	1	1

^aconcentrations (wt%) of V₂O₃ and VO₂ were calculated from original V₂O₃ data to yield stoichiometric formulae of the type A₂BO₅.

Table 3. Atomic coordinates and U_{eq}/U_{iso} of oxyvanite-berdesinskiite solid-solution members.

Position	<i>x</i>	<i>y</i>	<i>z</i>	U_{eq}/U_{iso}
Crystal I-2-7				
V1	0	0	0	0.00557(12)
V2	-0.12871(4)	-0.50005(8)	-0.21740(5)	0.00847(12)
O1	0.19284(16)	0.1544(3)	0.1536(2)	0.0102(3)
O2	0.08080(15)	-0.3434(3)	-0.0570(2)	0.0074(3)
O3	0	0.1931(4)	-1/4	0.0069(3)
Crystal II-7-21				
V1	0	0	0	0.00478(12)
V2	-0.12770(3)	-0.49833(7)	-0.21575(4)	0.00824(12)
O1	0.19284(13)	0.1550(3)	0.1520(2)	0.0091(2)
O2	0.08118(12)	-0.3431(3)	-0.05671(19)	0.0068(2)
O3	0	0.1926(4)	-1/4	0.0069(3)
III-7-22				
V1	0	0	0	0.0055(4)
V2	-0.12929(6)	-0.50103(7)	-0.21777(8)	0.0092(4)
O1	0.19176(18)	0.1552(4)	0.1544(3)	0.0101(5)
O2	0.0813(2)	-0.3446(4)	-0.0559(3)	0.0081(5)
O3	0	0.1936(5)	-1/4	0.0089(6)
III-9-11				
V1	0	0	0	0.0040(2)
V2	-0.13074(5)	-0.49931(10)	-0.22042(8)	0.0078(2)
O1	0.1906(2)	0.1557(5)	0.1572(3)	0.0092(5)
O2	0.0809(2)	-0.3439(4)	-0.0555(3)	0.0069(5)
O3	0	0.1953(6)	-1/4	0.0070(6)

Table 4. Atomic displacement parameters U_{ij} of oxyvanite-berdesinskiite solid-solution members.

	U_{11}	U_{22}	U_{33}	U_{23}	U_{13}	U_{12}
Crystal I-2-7						
V1	0.0070(2)	0.0042(2)	0.00645(19)	0.00075(18)	0.00368(14)	0.00085(16)
V2	0.01035(17)	0.00806(17)	0.00930(17)	0.00182(14)	0.00630(12)	0.00140(12)
O1	0.0090(6)	0.0086(6)	0.0121(6)	-0.0012(6)	0.0027(5)	-0.0008(5)
O2	0.0100(6)	0.0058(5)	0.0076(6)	-0.0016(5)	0.0048(5)	-0.0010(5)
O3	0.0094(8)	0.0050(8)	0.0080(8)	0.000	0.0051(6)	0.000
Crystal II-7-21						
V1	0.00507(18)	0.00406(18)	0.00521(18)	0.00068(16)	0.00184(13)	0.00083(12)
V2	0.00949(16)	0.00824(17)	0.00850(16)	0.00200(12)	0.00507(11)	0.00165(9)
O1	0.0068(5)	0.0082(5)	0.0102(6)	-0.0013(5)	0.0004(4)	-0.0002(4)
O2	0.0085(5)	0.0050(4)	0.0072(5)	-0.0010(4)	0.0033(4)	-0.0007(4)
O3	0.0078(6)	0.0064(7)	0.0068(7)	0.000	0.0032(6)	0.000
Crystal III-7-22						
V1	0.0056(6)	0.0063(6)	0.0047(6)	-0.00018(17)	0.0019(4)	-0.00038(17)
V2	0.0103(5)	0.0104(5)	0.0079(5)	-0.00129(13)	0.0045(3)	-0.00078(13)
O1	0.0089(11)	0.0103(11)	0.0099(11)	0.0006(6)	0.0022(8)	0.0009(6)
O2	0.0091(10)	0.0083(9)	0.0073(10)	-0.0008(6)	0.0033(7)	-0.0012(6)
O3	0.0110(13)	0.0102(13)	0.0065(12)	0.000	0.0042(10)	0.000
Crystal III-9-11						
V1	0.0044(4)	0.0034(4)	0.0044(4)	-0.0004(3)	0.0020(3)	-0.0002(3)
V2	0.0085(3)	0.0080(4)	0.0077(3)	-0.0004(2)	0.0041(2)	0.0005(2)

In the V_3O_5 structure type, including the minerals oxyvanite and berdesinskiite, these chains are stacked in a staircase-like arrangement (Fig. 1). Chain stacking is obtained by face-sharing of $M2O_6$ octahedra from adjacent chains and corner-sharing of $M1O_6$ octahedra. The

staircase-like fashion of the chains is also responsible for the monoclinic symmetry.

On the first glance one would rather expect that four-valent cations would avoid the M2 sites because of face-sharing with an adjacent $M2O_6$ octahedron.

Table 5. Interatomic M–O distances (Å) for oxyvanite-berdesinskiite solid-solution members.

M–O	I-2-7	II-7-21	III-7-22	III-9-11
M1–O1 2×	2.0014(15)	2.0055(9)	1.9888(18)	1.987(2)
M1–O3 2×	2.0031(11)	2.0099(13)	1.9998(15)	2.0054(15)
M1–O2 2×	2.0141(15)	2.0175(13)	2.017(2)	2.011(2)
Mean	2.006	2.011	2.002	2.001
M2–O1	1.8603(16)	1.8851(14)	1.8615(19)	1.854(2)
M2–O1	1.9668(17)	1.9635(15)	1.948(3)	1.943(2)
M2–O2	1.9697(16)	1.9686(14)	1.958(2)	1.968(2)
M2–O2	1.9740(15)	1.9778(15)	1.974(2)	1.976(2)
M2–O3	2.0816(16)	2.0909(15)	2.085(2)	2.077(2)
M2–O2	2.1450(15)	2.1457(13)	2.144(2)	2.163(2)
Mean	2.000	2.005	1.995	1.997

Face-sharing leads to close metal-metal contacts, which seem to be unfavourable for highly charged ions. On the other hand, the M1O₆ octahedron is very regular (center of symmetry) whereas the M2O₆ octahedron is extremely distorted both in angles and bond lengths (Fig. 2). In case of type-locality oxyvanite M1–O distances vary between 2.001 and 2.014 Å (Table 4) whereas M2–O distances range between 1.860 and 2.145 Å. Nonetheless, the average distances are very similar: $\langle \text{M1–O} \rangle = 2.006$ Å and $\langle \text{M2–O} \rangle = 2.000$ Å.

The structure exhibits three symmetry independent oxygen sites (O1, O2, and O3). O1 is three-coordinated by M sites whereas O2 and O3 are four-coordinated. As expected from bond-strength considerations O1 shows the shortest distances to adjacent M sites. In particular, the

distance M2–O1 is only 1.86 Å long whereas the opposite bond M2–O2 is the longest one with *ca.* 2.15 Å. Thus, the cation is displaced from the center of its coordination octahedron (Fig. 2). The out-of-center displacement is independent of whether the M₂O₆ octahedron carries V⁴⁺ or Ti⁴⁺ (this study; Hong & Åsbrink, 1982a). This is rather surprising because one would rather expect that Ti⁴⁺, as a d⁰ transition-metal ion, enhances the distortion due to development of a second-order Jahn-Teller effect (Kunz & Brown, 1995). Face-sharing of M₂O₆ octahedra occurs via common O2–O2–O3 octahedral faces with a separation of 2.78 Å between M2 sites.

Synthetic V₃O₅ exists in two closely related modifications. A low-temperature phase with complete V³⁺, V⁴⁺ order and space group *P2/c* is stable below 423–433 K (Åsbrink, 1980). Cation order leads to additional, very faint X-ray reflections violating *I*- or *C*-centering of space group No. 15. As a consequence of symmetry lowering, low-V₃O₅ exhibits four symmetry-independent metal sites; two sites have multiplicity 2, the remaining two have multiplicity 4 (general position). One site of general position is occupied by V⁴⁺ the other three are occupied by V³⁺. At higher temperature V₃O₅ preserves the same octahedral topology as the low-temperature phase but V⁴⁺ becomes disordered over two

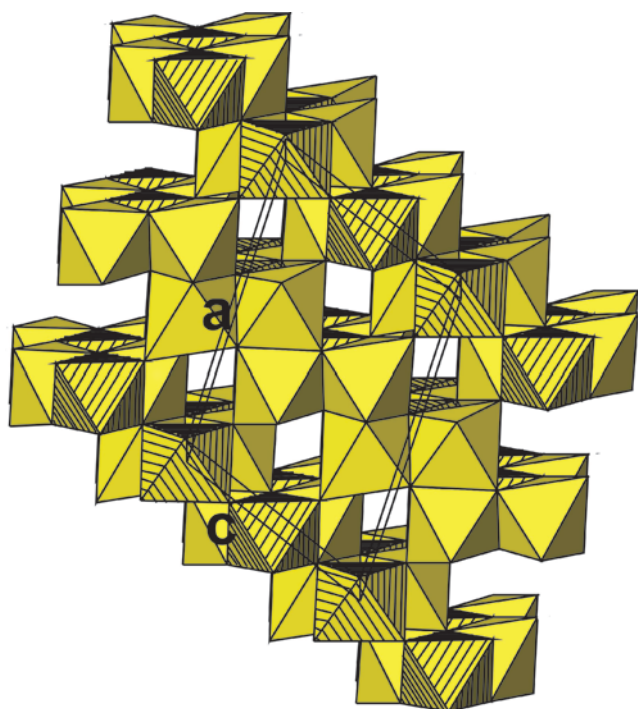


Fig. 1. Crystal structure of oxyvanite. M1O₆ octahedra occupied by three-valent cations are hatched. M2O₆ octahedra without hatching are occupied by both three- and four-valent cations.

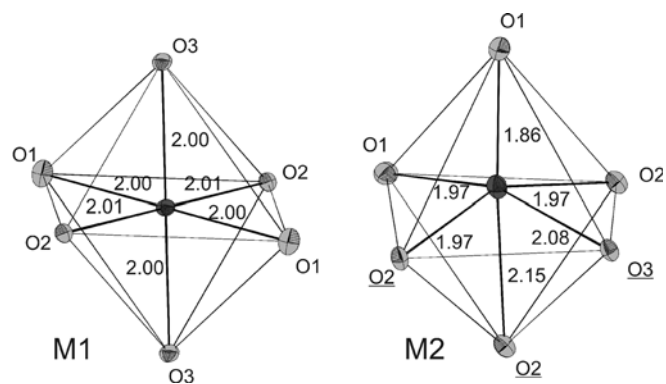


Fig. 2. Distortions of M1O₆ and M2O₆ octahedra: The M1O₆ octahedron has a center of symmetry at M1 whereas the M2O₆ octahedron is strongly distorted with the central cation displaced from the center of gravity. Underlined oxygen apices of the M2O₆ octahedron mark face-sharing triangles with an adjacent M2O₆ octahedron.

sites (Hong & Åsbrink 1982a). The phase transition has been described as a semiconductor-semiconductor or semiconductor-poor-metal transition. Hong & Åsbrink (1982a) argue that the V–V distances in high- and low- V_3O_5 are very similar excluding any metal-like effect for the high-temperature phase. However, in both phases the shortest V–V contacts are found between octahedra with different vanadium valence.

Schofield *et al.* (1995) summarized the possibilities of X-ray absorption spectroscopy investigated with synchrotron radiation in order to determine the valence of transition metals in minerals. The latter authors specifically address the cases of V^{2+} , V^{3+} , V^{4+} , and V^{5+} and provide various mineral examples of mixed V valence. Almost ten years before, Åsbrink *et al.* (1986) already applied XANES spectroscopy to synthetic V_2TiO_5 , isomorphous to V_3O_5 , to clarify whether the general position (multiplicity 8) is occupied by the ion pairs Ti^{3+} , V^{4+} or Ti^{4+} , V^{3+} and confidently assigned Ti^{4+} and V^{3+} to the distorted octahedrally coordinated site in the structure of V_2TiO_5 . Synthetic V_2TiO_5 corresponds in structure and composition to the rare mineral berdesinskiite (Bernhardt *et al.*, 1983).

We have not detected any violation of reflection conditions characteristic of C-centering for the studied solid-solution members between oxyvanite and berdesinskiite. However, the scattering power of the relatively small crystals investigated was probably not sufficient to exclude with certainty a low-temperature phase of primitive Bravais type (Åsbrink, 1980). On the other hand, at room temperature V_2TiO_5 does not exhibit corresponding complete Ti^{4+} order associated with symmetry reduction. Therefore, solid-solution members may follow the berdesinskiite-like trend in representing the centered Bravais type ($C2/c$ in our setting). The refined occupancies in our structure refinements are in full agreement with studies on synthetic V_2TiO_5 (Åsbrink *et al.*, 1986) where Ti^{4+} shares one distorted octahedral site with V^{3+} and a more regular octahedral site is occupied by mainly V^{3+} and Cr^{3+} .

Cr_2TiO_5 isomorphous with V_3O_5 and V_2TiO_5 has also been synthesized above 1660 °C in the system Cr_2O_3 – TiO_2 (Kamiya *et al.*, 1979). Koneva (2002) described rims around olkhonskite, $Cr_2Ti_3O_9$, of $(Cr,V)_2TiO_5$ with more than 50 % Cr_2TiO_5 component and established a solid-solution between berdesinskiite V_2TiO_5 and Cr_2TiO_5 for the metamorphic rocks of the Olkhon complex at Lake Baikal, Russia. Cr_2TiO_5 has not yet been accepted as mineral species. The solid-solution members studied by us also show 0.3 to 0.6 Cr^{3+} pfu substituting for V^{3+} .

Assuming linear relationship of cell dimensions (cell volume) (Kamiya *et al.*, 1979; Hong & Åsbrink, 1982a; Bernhardt *et al.*, 1983) in V_3O_5 – V_2TiO_5 – Cr_2TiO_5 solid-solution members, the following cell volumes may be predicted for the crystals investigated by us: I-2-7: 329.2 Å³, II-7-21: 330.5 Å³, III-9-11: 331.0 Å³. These unit-cell volumes predicted from end-members are in fair agreement with the measured volumes presented in Table 1. Judging from ionic radii given for octahedrally coordinated ions: V^{4+} : 0.58, Ti^{4+} : 0.60, Cr^{3+} : 0.615, V^{3+} :

0.64 Å (Shannon, 1976) berdesinskiite, V_2TiO_5 , should have a significantly larger cell volume than V_3O_5 and Cr_2TiO_5 , which is in agreement with volume data (336.4 Å³) by Bernhardt *et al.* (1983) for berdesinskiite.

Acknowledgement: Reviews by U. Kolitsch (Vienna, Austria) and R. Basso (Genoa, Italy) are highly acknowledged.

References

- Andersson, S., Sundholm, A., Magnéli, A. (1959): A homologous series of mixed titanium chromium oxides $Ti_{n-2}Cr_2O_{2n-1}$ isomorphous with the series Ti_nO_{2n-1} and V_nO_{2n-1} . *Acta Chem. Scand.*, **13**, 989–997.
- Armbruster, T., Kadiyski, M., Reznitsky, L.Z., Sklyarov, E.V., Galuskin, E.V. (2008): Batisivite, the first silicate related to the derbylite-hemloite group. *Eur. J. Mineral.*, **20**, 975–981.
- Åsbrink, S. (1980): The crystal structure and valency distribution in the low-temperature modification of V_3O_5 . The decisive importance of a few very weak reflexions in a crystal-structure determination. *Acta Crystallogr.*, **B36**, 1332–1339.
- Åsbrink, S., Greaves, G.N., Hatton, P.D., Garg, K. (1986): Reconciliation of valency ambiguity in V_2TiO_5 using XANES spectroscopy. *J. Appl. Crystallogr.*, **19**, 331–335.
- Bernhardt, H.-J., Schmetzer, K., Medenbach, O. (1983): Berdesinskiite, V_2TiO_5 , a new mineral from Kenya and additional data for schreyerite, $V_2Ti_3O_9$. *N. Jb. Mineral. Mh.*, **1983**, 110–118.
- Döbelin, N., Reznitsky, L.Z., Sklyarov, E.V., Armbruster, T., Medenbach, O. (2006): Schreyerite, $V_2Ti_3O_9$: new occurrence and crystal structure. *Am. Mineral.*, **91**, 196–202.
- Drofenik, M., Golič, L., Hanžel, D., Kraševc, V., Prodan, A., Bakker, M., Kolar, D. (1981): A new monoclinic phase in the Fe_2O_3 – TiO_2 system. I. Structure determination and Mössbauer spectroscopy. *J. Solid State Chem.*, **40**, 47–51.
- Enraf-Nonius (1983): Structure determination package (SDP), Enraf-Nonius, Delft, The Netherlands.
- Hong, S.H. & Åsbrink, S. (1982a): The structure of the high-temperature modification of V_3O_5 at 458 K. *Acta Crystallogr.*, **B38**, 713–719.
- , — (1982b): The structure of γ - Ti_3O_5 at 297 K. *Acta Crystallogr.*, **B38**, 2570–2576.
- Kamiya, S., Hirano, S., Somiya, S. (1979): The compound Cr_2TiO_5 in the system Cr_2O_3 – TiO_2 . *J. Solid State Chem.*, **28**, 21–28.
- Kolitsch, U. & Tillmanns, E. (2004): Does metastable monoclinic Sc_2TiO_5 exist? Insights from the crystal structures of berdesinskiite (V_2TiO_5) and an unnamed natural monoclinic Fe_2TiO_5 . Abstract volume 32nd International Geological Congress, Florence, Italy, August 20–28, G15.03.
- Koneva, A.A. (2002): Cr–V oxides in metamorphic rocks, Lake Baikal, Russia. *N. Jb. Mineral. Mh.*, **2002**, 541–550.
- Kunz, M. & Brown, I.D. (1995): Out-of-center distortions around octahedrally coordinated d^0 transition metals. *J. Solid State Chem.*, **115**, 395–406.
- Müller-Buschbaum, H. & Bluhm, K. (1988): Weitere magnetische Untersuchungen an $Ti_{(3-x)}M_{(x)}O_5$ -Phasen ($M = Al^{3+}$, Fe^{2+} , Mn^{2+} , Mg^{2+}) mit einem Beitrag über $CrTi_2O_5$. *Z. Anorg. Allg. Chem.*, **558**, 28–34.

- Papike, J.J., Karner, J.M., Shearer, C.K. (2004): Comparative planetary mineralogy: V/(Cr + Al) systematics in chromite as an indicator of relative oxygen fugacity. *Am. Mineral.*, **89**, 1557–1560.
- Reznitsky, L.Z., Sklyarov, E.V., Armbruster, T., Galuskin, E.V., Ushchapovskaya, Z.F., Polekhovsky, Yu.S., Karmanov, N.S., Kashaev, A.A., Barash, I.G. (2008): Batisivite, V₈Ti₆[Ba(Si₂O)]O₂₈, a new mineral species from the derbylite group. *Geol. Ore Deposits*, **50**, 7, 63–71.
- Reznitsky, L.Z., Sklyarov, E.V., Armbruster, T., Ushchapovskaya, Z.F., Galuskin, E.V., Yu.S., Polekhovsky, Barash, I.G. (in press): Oxyvanite, V₃O₅ – a new mineral, and isomorphous join oxyvanite – berdesinskiite V₂TiO₅ from metamorphic rocks of the Sludyanka complex (South Baikal region). *Proc. Russ. Mineral. Soc.*
- Schofield, P.F., Henderson, C.M.B., Cressey, G., Van der Laan, G. (1995): 2p X-ray absorption spectroscopy in the earth sciences. *J. Synchrotron Radiat.*, **2**, 93–98.
- Schuling, R.D. & Feenstra, A. (1980): Geochemical behaviour of vanadium in iron–titanium oxides. *Chem. Geol.*, **30**, 143–150.
- Shannon, R.D. (1976): Revised effective ionic radii and systematic studies of interatomic distances in halides and chalcogenides. *Acta Crystallogr.*, **A32**, 751–767.
- Sheldrick, G.M. (1997): SHELX-97, University of Göttingen, Germany.
- Wriedt, H.A. (1989): The O–V (oxygen–vanadium) system. *Bull. Alloy Phase Diagrams*, **10**, 271–277.

Received 23 December 2008

Modified version received 30 March 2009

Accepted 14 April 2009